Available online at www.sciencedirect.com
ScienceDirect
Journal of Power Sources 167 (2007) 243–249
JOURNAL OF POWER SOURCES
www.elsevier.com/locate/jpowsour

Carbon-supported Pd-Co bimetallic nanoparticles as electrocatalysts for the oxygen reduction reaction

Wenming Wang [a,b], Dan Zheng [a,b], Chong Du [a], Zhiqing Zou [a], Xigui Zhang [a], Baojia Xia [a], Hui Yang [a,*], Daniel L. Akins [c]

[a] *Energy Science and Technology Laboratory, Shanghai Institute of Microsystem and Information Technology, Chinese Academy of Sciences, Shanghai 200050, PR China*
[b] *Graduate University of the Chinese Academy of Sciences, Beijing 100039, PR China*
[c] *Center for Analysis of Structures and Interfaces, Department of Chemistry, The City College of The City University of New York, NY 10031, USA*

Received 9 November 2006; received in revised form 8 February 2007; accepted 8 February 2007
Available online 17 February 2007

Abstract

Carbon-supported Pd-Co bimetallic nanoparticle electrocatalysts of different Pd/Co atomic ratios were prepared by a modified polyol reduction. Electrocatalytic activities of the catalysts for the oxygen reduction reaction (ORR) have been investigated based on the porous rotating disk and disk-ring electrode techniques. As-prepared Pd-Co bimetallic nanoparticles evidence a single-phase fcc disordered structure, and the mean particle size is found to decrease with increase in Co content. A typical TEM image of the Pd_2Co/C catalyst, heat-treated at 500 °C, reveals a mean particle diameter is ca. 8.3 nm with a relatively narrow size distribution. For synthesized Pd-Co catalysts, the highest catalytic activity for the ORR, when supported on carbon (i.e., Pd-Co/C) was found for a Pd:Co atomic ratio of 2:1 and heat treatment at ca. 500 °C, corresponding to a Pd–Pd mean interatomic distance of ca. 0.273 nm. Kinetic analysis based on the rotating disk and disk-ring electrode measurements reveals that the ORR on Pd-Co/C catalysts undergoes a four-electron process in forming water. Because the Pd-Co/C catalyst is inactive for the adsorption and oxidation of methanol, it may function as a methanol-tolerant ORR catalyst in a direct methanol fuel cell.

Keywords: Pd-Co nanoparticle; Oxygen reduction reaction; Electrocatalysis; Methanol tolerance

1. Introduction

Proton exchange membrane fuel cells (PEMFCs), including the direct methanol fuel cell (DMFC), have received considerable attention for applications in the transportation arena, due to their high energy density, relatively low operating temperatures, zero or low emission of pollutants, and minimal corrosion problems [1–4]. However, the commercial viability of PEMFCs is still impacted by several problems, including poor kinetics of both the anodic and cathodic reactions and the high costs of Pt-based electrocatalysts [5,6]. Even under open-circuit condition, the overpotential for oxygen reduction in PEMFCs is around 0.2–0.3 V, due to irreversibility of the oxygen reduction reaction (ORR) and to the "mixed potential effect" that is caused by the competitive reaction between the adsorption of oxygen molecules on Pt surface and the formation of Pt oxide [7,8]. As a result, there proves substantial room for improvement in oxygen reduction kinetics. Indeed, extensive research for a number of decades has focused on the development of more active oxygen reduction catalysts as well as cheaper catalysts than Pt.

An additional issue is associated with a crossover phenomenon in which methanol penetrates from the anode, through the electrolyte membrane, to the cathode compartment, resulting in a significant loss in coulombic and voltage efficiencies of DMFCs when Pt/C is used as the cathodic catalyst; the main reason for the loss is oxidation of methanol at the cathode [9,10]. To avoid this problem, strategies include the development of novel, less methanol permeable membranes, possibly from modification of existing membranes [11,12]; the use of oxygen reduction catalysts that are inactive towards methanol oxidation or have a high methanol tolerance. Efforts in the later regard have involved the utilization of the ORR selective electrocatalysts, such as tran-

* Corresponding author. Tel.: +86 21 62511070; fax: +86 21 32200534.
E-mail address: hyang@mail.sim.ac.cn (H. Yang).

0378-7753/$ – see front matter © 2007 Elsevier B.V. All rights reserved.
doi:10.1016/j.jpowsour.2007.02.013

sition metalloporphyrins [13,14], transition metal sulfide [15], and Ru alloy [10,16]. However, the intrinsic catalytic activities of these catalysts for the reduction of oxygen are lower than that of Pt-based catalysts, and the long-term stability under fuel cell operating conditions at high potentials is also not as good as Pt-based catalysts. As a result, research dealing with the development of novel Pt-based electrocatalysts that can catalyze oxygen reduction but limit the oxidation of methanol has been of interest. And, indeed, several Pt alloy catalysts, in comparison to pure Pt, have exhibited a high methanol tolerance during the ORR [17,18]. However, the long-term stability of Pt alloy catalysts in a functioning DMFC is an anticipated fundamental issue since dissolution of non-noble metal components within the Pt nanosized alloy during fuel cell reactions would result in a significant decrease in methanol tolerance [19–21]. Therefore, it is highly desirable to develop new methanol-tolerant electrocatalysts that are more active for the ORR than catalysts that have been reported.

Efforts towards this latter end have involved catalysts containing Pd. Pd is more abundant and cheaper than Pt and its long-term stability in acidic media may be comparable with Pt; but its catalytic activity towards the ORR is several times lower than that for Pt and its alloys [22,23]. Recent reports, however, have shown that the catalytic activity of Pd-based catalysts for the ORR can be improved significantly by adding elements like Co, Ni, Cr, Fe, etc. Also, Pd-transitional metal alloy may be a good candidate as a methanol-tolerant ORR electrocatalyst in a DMFC because Pd catalyst is inactive for adsorption and oxidation of methanol [24–33]. Examples of works that support the use of Pd and its alloys as electrocatalysts include the following: (1) the report that sputtered Pd-transitional metal alloys exhibit a high catalytic activity and a good selectivity for the ORR in the absence and presence of methanol [24,33]; the authors suggest that the enhanced ORR activity of Pd-Co alloys might be attributed to an electronic stabilization of the added alloy element in the alloy. (2) It has been reported that Pd-based electrocatalysts with suitable metal combinations and optimum compositions exhibit high catalytic activity for the ORR; the ORR activity of the Pd-Co/C catalysts with a Co content of 10–30% is found to be close to that of Pt/C [25–28]; also, three carbon-supported Pd-based alloy electrocatalysts, Pd-Co-Au, Pd-Ti, and Pd-Co-Mo, have been prepared and their electrocatalytic activity is found to be comparable with Pt for the ORR in a PEMFC [28]. (3) $CoPd_3$/C electrocatalysts have been prepared by electrodeposition, and an enhanced ORR activity on such a catalyst in a 5 cm^2 PEMFC was found [29]. (4) Other investigators have analyzed the ORR kinetics of the CoPd system [30]; a similar ORR mechanism was found for both PdCo/C and Pt/C catalysts. And (5), recently, researchers have reported that carbon-supported Pd nanoparticles modified with Co became very active for the ORR [31,32]; these authors also reported that the catalytic activity of Pd_3Fe/C electrocatalyst prepared by thermal treatment surpassed that of the state-of-the-art Pt/C catalyst and that the enhanced catalytic activity is due to the more favorable Pd–Pd interatomic distance.

The particle size of Pd-based catalysts, as reported in literatures [25–28,32], is large, thus there proves to be significant room for improvement in ORR mass activity. Challenges to be met for the preparation of improved Pd alloy catalysts include the need for synthesis procedures resulting in catalysts with desirable composition, small particle size and a narrow size distribution. In the present paper, Pd-Co/C bimetallic catalysts with different atomic ratios were prepared by a modified polyol reduction process and then heat-treated at various temperatures, with the aim being to increase the ORR activity and to decrease the particle size of Pd-based catalysts. ORR activities were evaluated in an acid medium in the absence and presence of methanol. Also, ORR kinetics was analyzed, using a rotating disk electrode (RDE) as well as a rotating ring-disk electrode (RRDE).

2. Experimental

2.1. Catalyst preparation

The polyol reduction route has been employed previously for the preparation of Pt alloy nanoparticle catalysts [34,35]. Few studies dealing with preparation of Pd-based catalysts have been reported [36,37]. We have prepared in the present study Pd-Co/C catalysts by way of a modified polyol reduction synthesis. Briefly, the procedure involved mixing palladium chloride ($PdCl_2$) and cobalt chloride ($CoCl_2{\cdot}6H_2O$) ultrasonically in ethylene glycol (EG) solution. XC-72 carbon was then added under constant stirring. The Pd loading within the catalysts was controlled at a weight percent of 20 wt%; Co content was calculated according to Pd:Co atomic ratio of the desired product. NaOH in EG was then added to adjust the pH of the solution. Unless stated otherwise, the reaction temperature was kept at 100 °C for 6 h. The preparation process was conducted under flowing nitrogen. After cooling to room temperature, the mixture was filtrated, washed and dried at ca. 110 °C for more than 6 h. The resultant catalysts are denoted herein as as-prepared Pd-Co/C catalysts. The as-prepared Pd-Co/C catalysts were subsequently heat-treated at various temperatures between 400 and 700 °C in an atmosphere of flowing 10 vol% H_2–90 vol% N_2 for 2 h, then cooled to room temperature.

2.2. Physical characterization

The analysis of the composition of catalysts was performed with an IRIS Advantage inductively coupled plasma atomic emission spectroscopy (ICP-AES) system (Thermo, America). X-ray diffraction (XRD) measurements utilized a Rigaku D/MAX-2000 diffractometer with a Cu Kα radiation (1.54056 Å). The tube voltage was maintained at 40 kV and tube current at 100 mA. Diffraction patterns were collected from 10° to 90° at a scanning rate of 2° min^{-1}, and with a step size of 0.02°. The mean particle size, the lattice parameter and Pd–Pd interatomic distance were calculated from the (2 2 0) diffraction plane using the Scheerer equation and the Bragg equation, respectively [32]. The surface areas were estimated using an equation $S = 6000/rd$ [25–28], where r is the particle size in nm, obtained from the XRD data, and d is the density of the Pd-Co bimetallic catalyst. The density values used were 12.0 and 8.9 g cm^{-3} for Pd and Co, respectively. The sample for transmission electron microscopy (TEM) analysis was prepared by

ultrasonically suspending the catalyst powder in ethanol. A drop of the suspension was then placed onto a clean holey copper grid and dried under air. The morphology of the sample was characterized using a Technai G2 20s-Twin Microscope (FEP Inc., America) operated at 200 kV.

2.3. Electrochemical characterization

Porous electrodes were prepared as described previously [3,7]. Ten milligrams of Pd-Co/C catalysts, 0.5 mL of Nafion solution (5 wt%, Aldrich) and 2.5 mL of ultrapure water were mixed ultrasonically. A measured volume (ca. 3 μL) of this ink was transferred via a syringe onto a freshly polished glassy carbon disk (GC, 3 mm diameter). After the solvents were evaporated overnight at room temperature, the electrode was used as the working electrode. Each electrode contained ca. 28 μg cm^{-2} of Pd.

All chemicals were of analytical grade. All the solutions were prepared with ultrapure water with a specific resistance of >18 MΩ cm^{-1}. Electrochemical measurements were performed using an M 273A Potentiostat/Galvanostat (Princeton, USA) and a conventional three-electrode cell. The catalytic activity for the ORR was measured with a rotating disk electrode and a rotating ring-disk electrode mounted with a BM-ED 1101 electrode (Radiometer, France). The counter electrode was a glassy carbon plate, and a saturated calomel electrode (SCE) was used as the reference electrode. All potentials, however, are referenced with respect to the reversible hydrogen electrode (RHE). Prior to any electrochemical measurements, the porous electrodes were cycled between 0.05 and 1.00 V at a scan rate of 50 mV s^{-1} under N_2 until reproducible cyclic voltammograms (CVs) were obtained (ca. 15 cycles), in order to remove any contaminants from the electrode. The upper potential was set to ca.1.00 V so that any change in particle size could be avoided. High-purity nitrogen or oxygen was used for deaeration of the solutions. During the measurements, a gentle gas flow was kept above the electrolyte solution.

All experiments were carried out at a temperature of 25 ± 1 °C.

3. Results and discussion

3.1. Physical characterization of Pd-Co/C bimetallic catalysts

The practical composition of the Pd-Co/C catalysts was evaluated by ICP-AES analysis. The obtained ICP-AES compositions for all the catalysts are listed in Table 1. The practical compositions of the as-prepared Pd-Co/C bimetallic catalysts are found to be nearly the same as the stoichiometric values, indicating that Co may be alloyed with Pd for the modified polyol synthesis reduction procedure used.

Fig. 1a shows the XRD patterns of the as-prepared Pd-Co/C bimetallic catalysts, while Fig. 1b shows that for Pd_2Co/C catalysts heat-treated at various temperatures; for the sake of comparison, the Pd/C catalyst prepared by a similar procedure is also shown in Fig. 1a. As shown in Fig. 1a, all the XRD patterns

Table 1
Composition and structure of the Pd/C and Pd-Co/C bimetallic catalysts

Sample	Composition from ICP-AES (Pd:Co)	Particle size (nm)	Lattice parameter (nm)	S_{XRD} (m^2 g^{-1})
Pd/C	100	4.5	0.3895	111.1
Pd_4Co/C	81.3:18.7	3.0	0.3889	172.1
Pd_3Co/C	76.8:23.2	2.8	0.3888	186.0
Pd_2Co/C	62.9:37.1	2.6	0.3888	203.7
Pd_3Co_2/C	61.1:38.9	2.2	0.3885	244.3
PdCo/C	51.0:49.0	1.8	0.3877	305.9

clearly show five main characteristic peaks of face-centered-cubic (fcc) crystalline Pd, namely, the planes (1 1 1), (2 0 0), (2 2 0), (3 1 1) and (2 2 2), indicating that all the as-prepared catalysts mainly possess the single-phase fcc disordered structure (solid solution). The five diffraction peaks in Fig. 1a for the Pd-Co bimetallic catalysts are shifted slightly to higher 2θ values with respect to the corresponding peaks in the Pd/C catalyst, indicating the effect of increased amounts of Co in the Pd-Co bimetallic catalysts. In Fig. 1b, there are also five main diffraction peaks for fcc Pd_2Co/C catalysts heat-treated at various temperatures. With increase in heating temperature, these diffraction peaks shift to higher angle relative to pure Pd. Such angle shifts reveal alloy formation between Pd and Co with increase in heating temperature, and indicate lattice contractions,

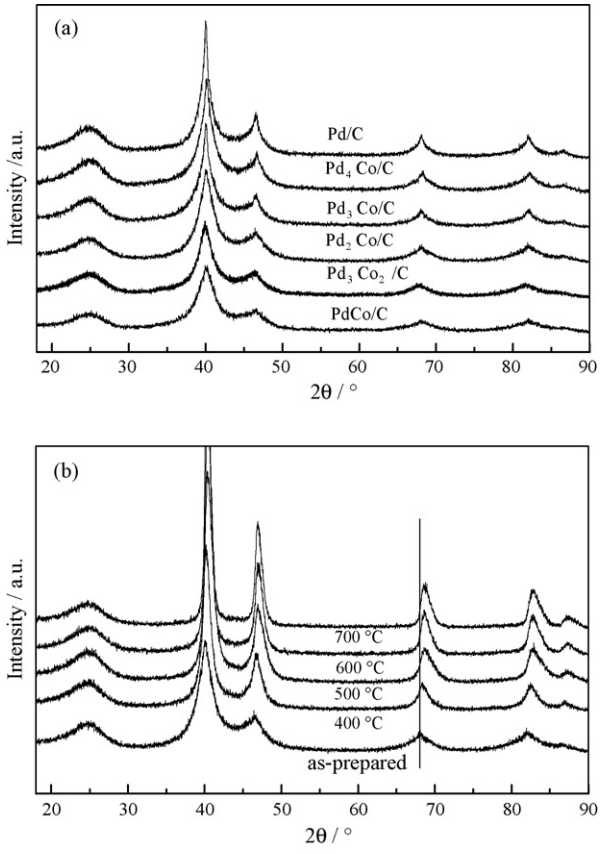

Fig. 1. X-ray diffraction patterns of (a) Pd/C and Pd-Co/C bimetallic catalysts prepared with polyol reduction and (b) the Pd_2Co/C alloy catalysts heat-treated in 10% vol-H_2 and 90% vol-N_2 atmosphere at various temperatures.

Table 2
Structural parameters of heat-treated Pd_2Co/C alloy catalysts

Sample	Particle size (nm)	Pd–Pd interatomic distance (nm)	Lattice parameter (nm)	S_{XRD} ($m^2\,g^{-1}$)
As-prepared	2.6	0.2750	0.3889	203.7
400 °C	6.4	0.2741	0.3876	108.1
500 °C	7.9	0.2732	0.3864	96.3
600 °C	9.6	0.2736	0.3869	72.6
700 °C	11.2	0.2739	0.3873	66.2

which are caused by the incorporation of Co into the Pd fcc structure. Angle shift increases and lattice parameter decreases with increase in heating temperature suggest an increased degree of alloying. Although no reflections corresponding to pure Co and its oxides are found, their presence may not be completely ruled out due to their smaller concentration levels and possibly poor crystallinity.

The mean particle sizes calculated from XRD patterns for all catalysts are shown in Tables 1 and 2. The mean particle size, as shown in Table 1, decreases with increase in Co content for the as-prepared catalysts; the lattice parameters of as-prepared Pd-Co bimetallic catalysts are also provided. The lattice parameters obtained for all the as-prepared Pd-Co/C catalysts are smaller than that of Pd/C and show a decrease with increase in Co content, indicative of a lattice contraction upon alloying. Additionally, as shown in Table 2, the average particle size for the Pd_2Co/C catalysts generally increases with heat-treatment temperature; the Pd–Pd interatomic distances of the Pd_2Co/C catalysts are also provided. The minimum Pd–Pd interatomic distance for the Pd_2Co/C catalysts is found to be ca. 0.273 nm at a heat treatment temperature of 500 °C.

The XRD-determined surface areas (S_{XRD}) are also provided in Tables 1 and 2. As indicated in Table 1, S_{XRD} increases with Co content for the as-prepared catalysts. However, S_{XRD} in Table 2 is shown to decrease at higher heat treatment temperatures for the Pd_2Co/C alloy, attributed to the increase in particle size.

Fig. 2 shows a typical TEM image of a Pd_2Co/C catalyst heat-treated at 500 °C and the corresponding particle size distribution histogram based on the observation of more than 300 nanoparticles. As can be seen, the Pd_2Co alloy nanoparticles are well dispersed on the surface of the support with a relatively narrow particle size distribution, and the mean particle size is about 8.3 ± 3.1 nm in diameter, which is in fairly good agreement with the data calculated from XRD. The ascertained mean particle size is smaller than those reported by others for Pd-based catalysts, which may be beneficial for increasing in the ORR mass activity. Hence, the catalyst preparation procedure via a modified polyol reduction route may be a method for obtaining nanosized alloy catalysts with a narrow particle distribution and a good dispersion on a support.

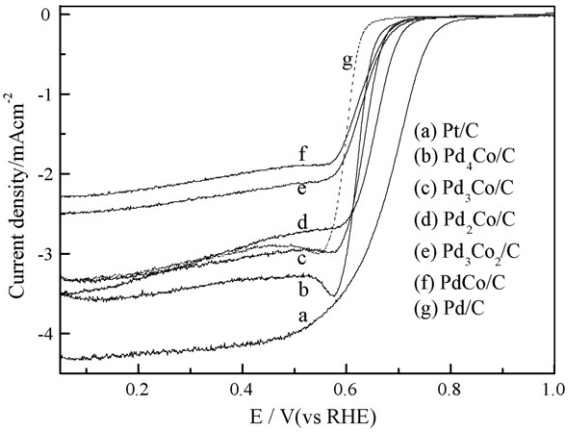

Fig. 3. Linear scan voltammgrams (LSVs) of Pt/C catalyst, and as-prepared Pd/C and Pd-Co/C bimetallic catalysts prepared with only polyol reduction in 0.1 M $HClO_4$ saturated with pure oxygen at a scan rate of 5 mV s^{-1} and with a rotation speed of 1600 rpm. Current density is normalized to the geometrical surface area of the electrode.

3.2. Electrochemical characterization of the Pd-Co/C bimetallic catalysts

Fig. 3 is a comparison of the ORR on Pt/C and as-prepared Pd-Co/C bimetallic catalysts under similar experimental conditions. For the sake of comparison, the ORR on the Pd/C catalyst pre-

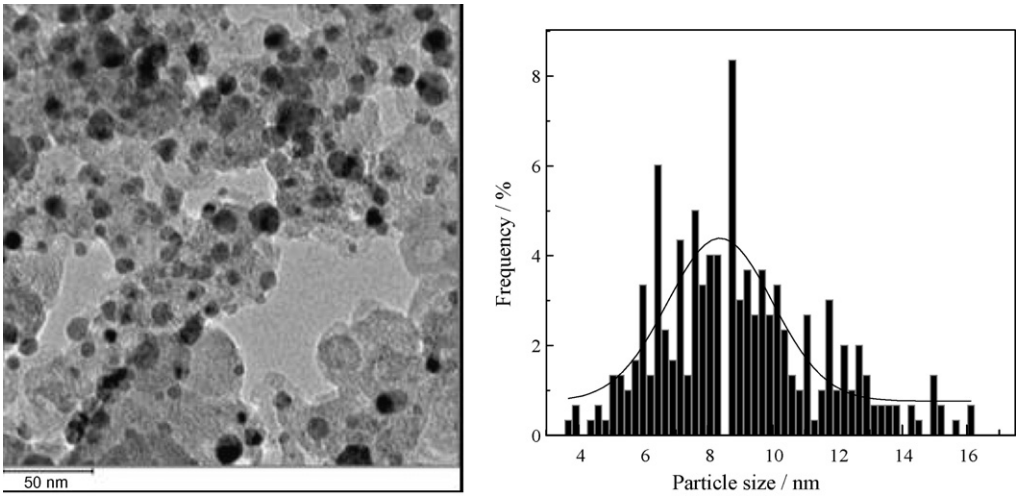

Fig. 2. TEM image and the corresponding particle size distribution histogram of Pd_2Co/C catalyst heat-treated at 500 °C.

pared by a similar procedure is also shown in the figure. From the figure, the ORR on all the catalysts is diffusion-controlled when the potential is less than 0.55 V, and is under mixed diffusion-kinetic control in the potential region between 0.55 and 0.80 V. When the potential is higher than 0.80 V, the ORR is under kinetic control in the Tafel region. It is worth mentioning that the limiting current density decreases with increase in Co content (for the as-prepared Pd-Co/C bimetallic catalysts), probably due to the difference in the hydrophilic/hydrophobic behavior of the catalysts. As can be seen, all the as-prepared Pd bimetallic catalysts exhibited lower ORR overpotential than the Pd/C catalyst, assessing that the alloying of Pd with Co leads to an increased ORR activity. In the kinetic and mixed regions, the highest catalytic activity for the ORR among all the Pd-based catalysts was found with a Pd:Co atomic ratio of 2:1. However, the ORR overpotential on all of the Pd-based catalysts is higher than that on the Pt/C catalyst, indicating that the ORR activity on Pd-based catalysts is lower than that on the Pt-based catalysts in pure acidic solution.

Fig. 4 shows a comparison of the ORR on the Pt/C and Pd_2Co/C alloy catalysts that were heat-treated at various temperatures under similar experimental conditions. One can see that the maximum catalytic activity for the Pd_2Co/C alloy catalysts is found at a heat treatment temperature of 500 °C, indicating that the heat treatment of the catalysts has a significant influence on ORR activity. The increase in catalytic activity for the catalysts treated from 400 to 500 °C is probably due to an increase in the degree of alloying, while the decrease in catalytic activity from 500 to 700 °C may be due to an increase in particle size. It is known that both geometric and electronic parameters are two key factors in determining the chemisorption behavior of oxygenated species and catalytic activity for the ORR [7,28]. The relationship between kinetic current density (J_k) at 0.75 V (versus RHE) and Pd–Pd interatomic distance is plotted in Fig. 5. A nearly linear correlation is observed between J_k and the Pd–Pd interatomic distance as a function of the heat treatment temperature.

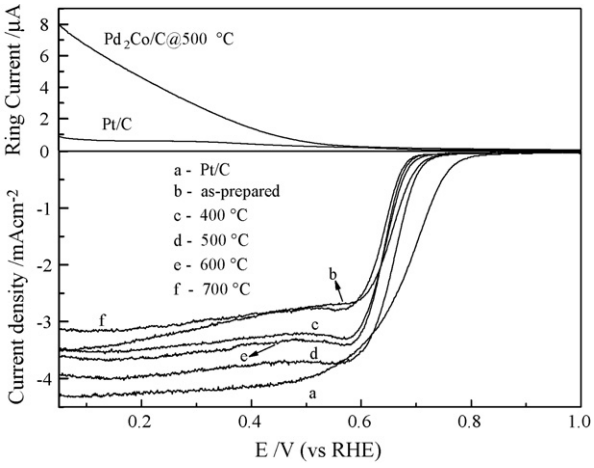

Fig. 4. LSVs of the Pt/C and Pd_2Co/C catalysts heat-treated in 10% H_2–90% N_2 atmosphere at various temperatures in 0.1 M $HClO_4$ saturated with pure oxygen. The other conditions are identical to those of Fig. 3. Current density is normalized to the geometrical surface area of the electrode. The ring currents, RRDE data, for hydrogen peroxide production are compared.

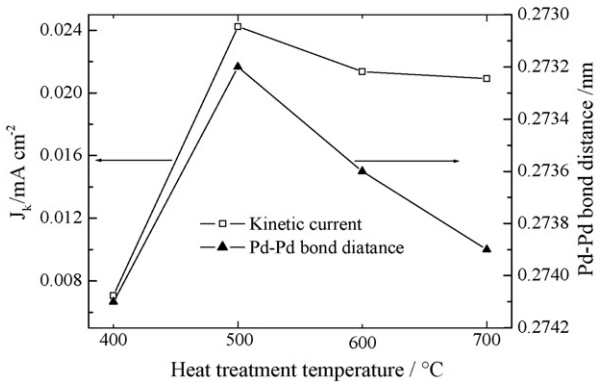

Fig. 5. Effect of heat treatment temperature on the kinetic current density at 0.75 V for the Pd_2Co/C catalyst. Pd–Pd interatomic distance calculated from XRD data.

The largest value for the ORR activity for Pd_2Co/C catalysts is obtained at a heat treatment temperature of 500 °C, corresponding to a Pd–Pd interatomic distance of ca. 0.273 nm. In general, the activity enhancement for the ORR on Pt-based alloy catalysts is attributable to changes in Pt mean interatomic distance and Pt-M composition. As reported [3,38,39], the appropriate Pt–Pt mean interatomic distance for adsorption and reduction of oxygen is between 0.271 and 0.275 nm; by coincidence, the Pd–Pd mean interatomic distance of a Pd_2Co/C treated at 500 °C is located in this range. For the Pd-based catalysts, it has been reported that the highest ORR activity of Pd-Fe/C alloy electrocatalysts is obtained with a Pd–Pd interatomic distance of 0.273 nm [32]. Consequently, it is likely that the high ORR activity that we have found for the (heat-treated at 500 °C) Pd_2Co/C catalyst is associated with an optimal Pd–Pd interatomic distance for the adsorption and reduction of oxygen.

RRDE data shown in Fig. 4 are also illustrative of the ORR pathway [$4e^-$ (water formation) or $2e^-$ (hydrogen peroxide formation)] on the Pt/C catalyst and Pd_2Co/C alloy catalyst heat-treated at 500 °C. The ring current is found to be negligible compared to the disk current for potentials above 0.6 V, indicating that the ORR proceeds without peroxide production. The ring current monotonicallly increases, starting from potentials lower than 0.6 V, and the amount of peroxide formed on the Pd_2Co/C alloy catalyst is higher than that formed on pure Pt. The fraction of peroxide, $X_{H_2O_2}$, at a typical fuel cell operating potential of 0.70 V/RHE, was evaluated from disk current (I_D), ring current (I_R) and collection factor ($N = 0.20$) using the equation: $X_{H_2O_2} = 2I_R/N/(I_D + I_R/N)$ [3,7]. The fractions are 0.22 and 0.84% for the Pt/C and Pd_2Co/C catalysts, respectively. Thus, the ORR reveals negligible peroxide production on the Pd_2Co/C alloy catalyst while the ORR on the Pd_2Co/C alloy catalyst indicates a four-electron process leading to water formation.

Fig. 6 shows LSVs of the Pd_2Co/C catalyst heat-treated at 500 °C in 0.1 M $HClO_4$ electrolyte saturated with pure oxygen at different rotation speeds. It can be seen that the ORR activity in the kinetic region is essentially the same at the different speeds. In the mixed and diffusion-controlled regions, the catalytic current depends on the rotation speed. Fig. 7 shows

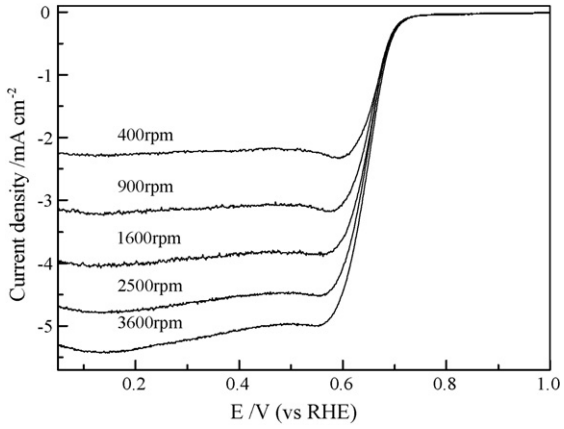

Fig. 6. LSVs of the Pd_2Co/C catalyst heat-treated at 500 °C in 0.1 M $HClO_4$ saturated with pure oxygen at a scan rate of 5 mV s^{-1}, at different rotation speeds. Current density is normalized to the geometrical surface area of the electrode.

selected Koutecky–Levich plots obtained for the catalyst, heat-treated at 500 °C. All plots in Fig. 7 are nearly straight lines within the fitting error, indicating a first-order oxygen reduction reaction. From the Koutecky–Levich equation $I^{-1} = I_k^{-1} + (0.62nFD^{2/3}Cv^{-1/6}\omega^{1/2})^{-1}$ and the measured slopes, the apparent number of electrons transferred per oxygen molecule on the catalyst can be calculated. To calculate the Levich constant, we used a bulk O_2 solubility of 1.18×10^{-6} mol cm^{-3}, a diffusion coefficient of 1.9×10^{-5} cm^2 s^{-1} and a kinematic viscosity of 8.93×10^{-3} cm^2 s^{-1} for $HClO_4$ solution [40]. Calculated results reveal that the ORR on the Pt/C and Pd-Co/C catalysts undergoes a four-electron process to water, in good agreement with RRDE results.

It is well known that the crossover of methanol from the anode to the Pt cathode can lead to a further reduction in cell voltage, by ca. 200–300 mV. There is a competitive reaction between oxygen reduction and methanol oxidation on Pt-based cathodes. Thus, it is highly desirable to develop selective-ORR electrocatalysts that have a high methanol tolerance for DMFC applications. Fig. 8 shows ORR on the Pt/C and Pd_2Co/C alloy catalyst heat-treated at 500 °C in 0.1 M $HClO_4$ solution, in the absence and presence of 1 M CH_3OH saturated with pure oxygen. For the ORR on pure Pt catalyst in methanol-containing solution, the overpotential increases by ca. 200 mV. The significant increase in overpotential of the ORR on pure Pt catalyst is due to the competitive reaction between oxygen reduction and methanol oxidation. By using the Pd-Co alloy catalyst, there is also an activity decrease for the ORR in methanol-containing electrolyte. However, the potential loss on such Pd-Co catalyst is ca. 15 mV in comparison to that in pure acid solution. From the figure, it is very clear that the ORR activity on the Pd-Co alloy catalyst in methanol-containing solution is much higher than that on pure Pt, indicating that Pd_2Co/C exhibits a high ORR selectivity in the presence of methanol in acid medium. Furthermore, all the Pd-Co/C catalysts were found to exhibit the same characteristics as the Pd_2Co/C alloy for the adsorption and oxidation of methanol. As is well known, Pd is inactive for the adsorption and oxidation of methanol, and the addition of Co to Pd has been found to have no effect on adsorption and oxidation of methanol. Hence, the Pd-Co/C catalyst represents a new and promising type of catalyst for selective-ORR in a DMFC.

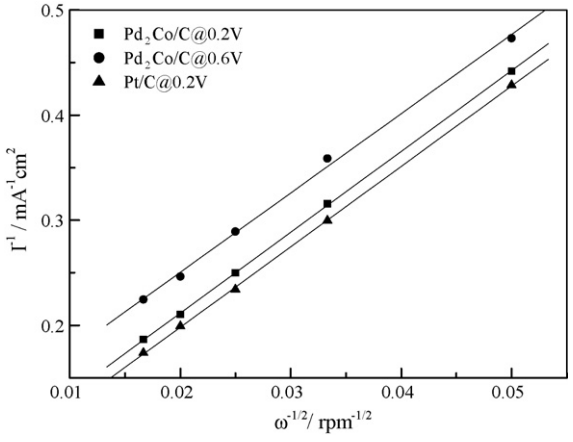

Fig. 7. Koutechy–Levich plots for the ORR in 0.1 M $HClO_4$ on the Pt/C and Pd_2Co/C catalysts heat-treated at 500 °C. Current density is normalized to the geometric surface area of the electrode.

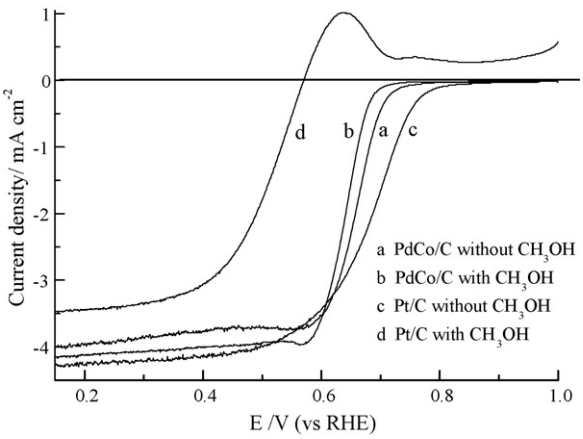

Fig. 8. LSVs of oxygen reduction on the Pd_2Co/C alloy catalyst heat-treated at 500 °C and the commercial Pt/C catalyst in 0.1 M $HClO_4$ solution in the absence and presence of 1 M CH_3OH saturated with pure oxygen. Other conditions are identical to those of Fig. 3.

4. Conclusions

Carbon-supported Pd-Co bimetallic nanoparticles of relatively small particle size and single-phase fcc disordered structure have been prepared via a modified polyol reduction, followed by a heat treatment at evaluated temperatures. For the as-prepared Pd-based catalysts, the observed maximum ORR activity was found with a Pd/Co atomic ratio of 2:1 and for heat treatment temperature of 500 °C. The enhanced catalytic activity of the Pd_2Co/C may be ascribed to the Pd–Pd having, as a result of the synthesis method, by coincidence an appropriate interatomic distance for the adsorption and reduction of molecule oxygen. Furthermore, Pd-Co/C catalysts have a very good ORR selectivity in the presence of methanol. Thus, Pd-Co/C catalyst may be a new, promising catalyst for the selective-ORR in a DMFC. Further investigations, including a comparison of the ORR activity of Pd-Co/C catalysts with different atomic ratios,

with heat treatment at the same temperature, and a range of particle sizes is underway.

Acknowledgments

H.Y. thanks the National Natural Science Foundation of China (20673136), the National Defense Fundamental Foundation of China (A1320070025), the National "863" High-Technology Research Program of China (2006AA05Z136, 2006AA04Z342), the 100 People Plan Program of Chinese Academy of Sciences and the Pujiang Program of Shanghai City (No. 06PJ14110) for support of this work. DLA thanks the NSF and DoD-ARO for support of this work, in part, through the following awards: (1) the NSF-MRSEC program under grant DMR-0213574; the (2) NSF-NSEC program under grant CHE-06-41523; and (3) DoD-ARO under Cooperative Agreement DAAD19-01-1-0759 and grant W911NF-04-1-0029.

References

[1] B.D. Mcnicol, D.A.J. Rand, K.R. Williams, J. Power Sources 83 (1999) 15.
[2] E. Antolini, J.R.C. Salgado, E.R. Gonzalez, J. Electroanal. Chem. 580 (2005) 145.
[3] H. Yang, W. Vogel, C. Lamy, N. Alonso-Vante, J. Phys. Chem. B 108 (2004) 11024.
[4] V.S. Murthi, R.C. Urian, S. Mukerjee, J. Phys. Chem. B 108 (2004) 11011.
[5] T.D. Jarvi, S. Stuve, E.M. Sriramulu, J. Phys. Chem. B 101 (1997) 3646.
[6] T.R. Ralph, M.P. Hogarth, Platinum Met. Rev. 46 (2002) 3.
[7] H. Yang, N. Alonso-Vante, J.J.-M. Léger, C. Lamy, J. Phys. Chem. B 108 (2004) 1938.
[8] X. Wang, M. Waje, Y.S. Yan, J. Electrochem. Soc. 151 (2004) A2183.
[9] (a) R.Z. Jiang, D.Y. Chu, J. Electrochem. Soc. 147 (2000) 4605;
(b) P. Convert, C. Coutanceau, F. Claguen, C. Lamy, J. Appl. Electrochem. 31 (2001) 945.
[10] T.J. Schmidt, U.A. Paulus, H.A. Gasteiger, N. Alonso-Vante, R.J. Behm, J. Electrochem. Soc. 147 (2000) 2620.
[11] J.A. Kerres, J. Membr. Sci. 185 (2001) 3.
[12] Z.Q. Ma, P. Cheng, T.S. Zhao, J. Membr. Sci. 215 (2003) 327.
[13] J. Fournier, G. Lalande, R. Cote, D. Guay, J.P. Dodelet, J. Electrochem. Soc. 144 (1997) 218.
[14] S.Lj. Gojkovic, S. Gupta, R.F. Savinell, J. Electroanal. Chem. 462 (1999) 63.
[15] R.W. Reeve, P.A. Christensen, A.J. Dickinson, A. Hamnett, K. Scott, Electrochim. Acta 45 (2000) 4237.
[16] N. Alonso Vante, H. Tributsch, Nature 323 (1986) 431.
[17] E. Antolini, J.R.C. Salgado, E.R. Gonzalez, J. Power Sources 155 (2006) 161.
[18] H.A. Gasteiger, S.S. Kocha, B. Sompalli, F.T. Wagner, Appl. Catal. B: Environ. 56 (2005) 9.
[19] A. Bonakdarpour, J. Wenzel, D.A. Stevens, S. Sheng, T.L. Monchesky, R. Lobel, R.T. Atanasoski, A.K. Schmoeckel, G.D. Vernstorm, M.K. Debe, J.R. Dahn, J. Electrochem. Soc. 151 (2005) A61.
[20] T. Toda, H. Igarashi, H. Uchida, M. Watanabe, J. Electrochem. Soc. 146 (1999) 3750.
[21] H.R. Colon-Mercado, H. Kim, B.N. Popov, Electrochem. Commun. 6 (2004) 795.
[22] P. Pattabiraman, Appl. Catal. A 153 (1997) 9.
[23] M.T. Giacomi, M. Balasubramanian, S. Khalid, J. McBreen, J. Electrochem. Soc. 150 (2003) A593.
[24] O. Savadogo, K. Lee, K. Oishi, S. Mitsushima, N. Kamiya, K.I. Ota, Electrochem. Commun. 6 (2004) 105.
[25] J.L. Fernandez, D.A. Walsh, A.J. Bard, J. Am. Chem. Soc. 127 (2005) 357.
[26] J.L. Fernandez, V. Raghuveer, A. Manthiram, A.J. Bard, J. Am. Chem. Soc. 127 (2005) 13100.
[27] V. Raghuveer, A. Manthiram, A.J. Bard, J. Phys. Chem. B 109 (2005) 22909.
[28] V. Raghuveer, P.J. Ferreira, A. Manthiram, Electrochem. Commun. 8 (2006) 807.
[29] W.E. Mustain, K. Kepler, J. Prakash, Electrochem. Commun. 8 (2006) 406.
[30] M.R. Tarasevich, A.E. Chalykh, V.A. Bogdanovskaya, L.N. Kuznetsova, N.A. Kapustina, B.N. Efremov, M.R. Ehrenburg, L.A. Reznikova, Electrochim. Acta 21 (2006) 4455.
[31] T. Huang, P. Liu, J. Zhang, R.R. Adzic, The 207th Electrochemistry Society Meeting, vol. 501, 2006, p. 1588.
[32] M.H. Shao, K. Sasaki, R.R. Adzic, J. Am. Chem. Soc. 128 (2006) 3526.
[33] K. Lee, O. Savadogo, A. Ishihara, S. Mitsushima, N. Kamiya, K. Ota, J. Electrochem. Soc. 153 (2006) A20.
[34] W.Z. Li, C.H. Liang, W.J. Zhou, J.S. Qiu, Z.H. Zhou, G.Q. Sun, Q. Xin, J. Phys. Chem. B 107 (2003) 6292.
[35] W.Z. Li, C.H. Liang, J.S. Qiu, W.J. Zhou, H.M. Han, Z.B. Wei, G.Q. Sun, Q. Xin, Carbon 40 (2002) 787.
[36] Z.H. Zhou, S.L. Wang, W.J. Zhou, G.X. Wang, L.H. Jiang, W.Z. Li, Chem. Commun. 1 (2003) 394.
[37] L.J. Chen, C.C. Wan, Y.Y. Wang, J. Colloid Interface Sci. 297 (2006) 143.
[38] S. Mukerjee, S. Srinivasan, M.P. Soriaga, J. Phys. Chem. B 99 (1995) 4577.
[39] M.K. Min, J. Cho, K. Cho, H. Kim, Electrochim. Acta 45 (2000) 4211.
[40] U.A. Paulus, A. WoKaun, G.G. Scherer, T.J. Schmidt, V. Stamenkovic, V. Radmilovic, N.M. Markovic, P.N. Ross, J. Phys. Chem. B 106 (2002) 4181.